

Quantized conductance in Au-Pd and Au-Ag alloy nanocontacts

Akihiro Enomoto,* Shu Kurokawa, and Akira Sakai†

Mesoscopic Materials Research Center, Kyoto University, Sakyo-ku, Kyoto 606-8501, Japan

(Received 16 August 2001; revised manuscript received 1 November 2001; published 12 March 2002)

We measure the quantized conductance in Au-Pd and Au-Ag alloy nanocontacts for a wide range of Pd and Ag concentrations, and study how the $1G_0$ conductance of Au changes with alloying. In Au-Pd, the $1G_0$ peak in a conductance histogram decreases in height with increasing Pd concentration, and disappears at around 80-at.% Pd. The $1G_0$ peak shows no peak shift and forms no subpeaks upon Pd alloying. This result indicates that the $1G_0$ conductance in Au-Pd nanocontacts is due to an all-Au atomic link connecting electrodes. Assuming a simple contact geometry, we calculate the formation probability of a Au link as a function of the Pd concentration, and find good agreement with the concentration dependence of the $1G_0$ peak height. On the other hand, in Au-Ag, the $1G_0$ peak can be observed for an entire range of Ag concentration, and its peak height changes as a linear compositional average of those of pure Au and Ag.

DOI: 10.1103/PhysRevB.65.125410

PACS number(s): 73.40.Jn, 73.63.Rt, 73.63.Nm, 68.65.La

I. INTRODUCTION

The quantization of conductance in metal nanocontacts is best observed in Au nanocontacts.¹ When a Au contact breaks, its conductance decreases stepwise, showing well-defined plateaus at integer multiples of the conductance quantum $G_0=2e^2/h$. Also, a conductance histogram constructed from many such conductance data shows a sharp peak at $1G_0$ and small subpeaks at $2G_0, 3G_0, \dots$.²⁻⁴ A clear $1G_0$ peak is also observed in conductance histograms of Ag and Cu,^{4,5} though $2G_0$ and higher conductance peaks are less clear in these metals. Conductance calculations⁶⁻⁸ and experiments⁹ showed that the $1G_0$ conductance in Au is due to a highly transmitting *sp* channel at the Fermi level. Compared to noble metals, on the other hand, transition-metal nanocontacts show less clear evidence of conductance quantization. Some workers found well-defined nG_0 (or $nG_0/2$) peaks in Fe and Ni,¹⁰⁻¹³ but others did not.^{4,5,14,15} Our previous experiments¹⁶ on Pd, Pt, Rh, Ru, and Ir showed that none of these metals exhibit clear nG_0 peaks in their histograms. Instead, we found broad and nonquantized peaks in conductance histograms of Pt, Ru, and Rh. No peaks were observed in Pd and Ir. Since Pd is as soft as Cu, the absence of quantized conductance in Pd is not due to its mechanical hardness, but may be related to its *d*-state valence electrons, the conductance channel of which do not exhibit clear quantization.^{7,17} As to the appearance of the quantized conductance, therefore, Au and Pd nanocontacts represent two opposite extremes; the most positive and negative examples. An interesting issue then is the quantized conductance in a mixture of these two elements, i.e., Au-Pd alloys. How does the quantized conductance in Au nanocontacts change upon alloying with Pd? Does it disappear by a small addition of Pd, or survive even in Pd-rich alloys?

At this time, little experimental and theoretical information is available about the conductance of alloy nanocontacts. Hansen *et al.*⁴ measured the conductance of Au-5-wt.%Cu nanocontacts, and observed the same nG_0 peaks as those in pure Au. They attributed these peaks to nanocontacts entirely made up of Au atoms. No other experiments were reported on alloy nanocontacts. García-Mochales and Serena,¹⁸ and

also Bürki *et al.*¹⁹ calculated the conductance of disordered nanocontacts, and showed that the electron scattering by random impurities shifts nG_0 peaks to lower values and reduces their peak height. Their calculations were, however, limited to small impurity concentrations (a few percent), and more concerned with “residual” (or lead) resistance¹⁸ than alloying effects. A strong impurity scattering was predicted by Brandbyge *et al.*,²⁰ who showed that an electron scatterer located at the center of a nanocontact almost washes out the $1G_0$ conductance peak. These calculations were made on model nanocontacts, and were not specific to contact materials. On the other hand, Lang²¹ theoretically studied how conductance changes when a foreign atom is inserted into a single-atom chain. He found that the conductance of a three-atom Al chain decreases by a factor of 1/4 when a center Al atom is replaced by an S (sulfur) atom. This conductance reduction takes place because the inserted S atom has a small *p*-state density at the Fermi level, and effectively shuts off *p* conductance channels of Al. Since Pd atoms in Au-Pd also have a small *sp* state density at the Fermi level,^{22,23} it is naturally expected from Lang’s calculations that a Pd atom acts as a bottleneck of the *sp* conductance channel of Au, and hence suppresses the quantized conductance when it occupies a contact site. However, such an alloying effect has not been studied experimentally. In this paper we report our experimental results on the conductance of Au-Pd alloy nanocontacts. We measured the conductance of Au-Pd alloy nanocontacts over a wide range of Pd concentrations, and observed how the conductance histogram changes upon alloying with Pd. We also carried out similar conductance measurements on Au-Ag alloy nanocontacts. Different from Pd, Ag shows a quantized conductance, and displays a clear $1G_0$ peak in its conductance histogram. A comparison of the results on Au-Pd and Au-Ag will make it clear how alloying effects depend on the characteristics of solute atoms.

II. EXPERIMENT

Conductance measurements were carried out on Au-Pd alloy wires with 17, 32, 55, 65, 88, and 97 at.%Pd, and Au-Ag alloy wires with 31, 55, 73, and 88 at.%Ag. We made

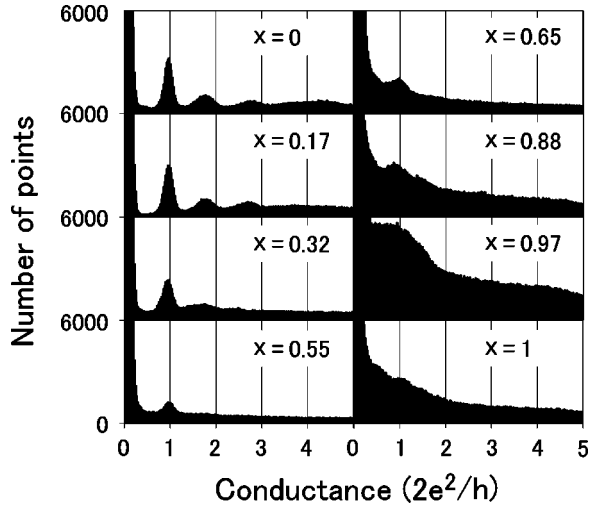


FIG. 1. Conductance histograms of $\text{Au}_{1-x}\text{Pd}_x$ obtained at 200 mV.

and broke a contact between two wires by moving one wire against another fixed wire. A piezo actuator, attached to a linear translator for a coarse approach, was used for moving the wire. We applied a small sinusoidal voltage to the piezo actuator, and adjusted the wire position so that the contact repeats on-off cycles. The maximum retracting speed of the wire was 0.25 mm/s. The transient conductance during the contact break was recorded by a fast digital oscilloscope. Details of conductance measurements are described elsewhere.^{16,24,25} All measurements were carried out at room temperature in vacuum of $\sim 3 \times 10^{-3}$ Pa. We note that our contacts were formed by firmly pressing a wire against another one, and hence a “hard indentation” type described by Hansen *et al.*⁸ As well explained in Ref. 8, the conductance of a hard-indentation contact is less sensitive to contamination than that of a soft-touching contact, since a surface contamination layer is broken during a contact formation. Also, since the last stage of the contact break, in which a nanocontact is formed, usually completes within less than 10 μs , a probability of attaching gas molecules to a fresh nanocontact is estimated to be small even in low vacuum. For example at 3×10^{-3} Pa, the number of gas molecules hitting a contact surface of $1 \times 1 \text{ nm}^2$ during 10 μs becomes $\leq 1 \times 10^{-3}$. Therefore, we believe that our nanocontacts remained contamination free, at least during a short period of time just before they break off.

III. RESULTS

A. Au-Pd contacts

We carried out conductance measurements, varying the bias voltage from 200 mV to 1.0 V in 200-mV step. To separate alloying effects from high-bias effects,^{24,25} however, we will not discuss high-bias data, and will concentrate on our conductance data obtained at 200 mV. Figure 1 shows conductance histograms of $\text{Au}_{1-x}\text{Pd}_x$ obtained at 200 mV for different alloy compositions. Histograms of pure Au and Pd are also shown for comparison. Each histogram was constructed from 2000 conductance traces. It can be seen clearly

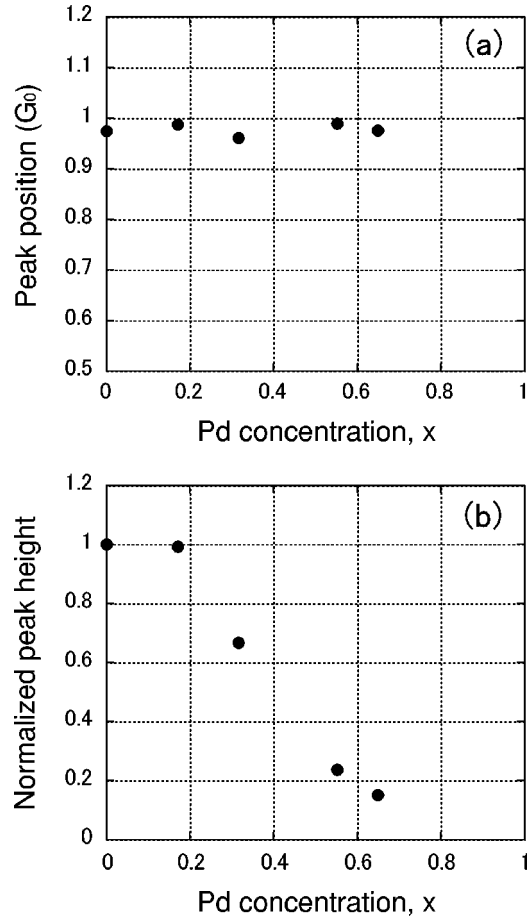


FIG. 2. Peak position (a) and peak height (b) of the $1G_0$ conductance peak of $\text{Au}_{1-x}\text{Pd}_x$ plotted against the Pd concentration. The peak height is normalized by its value at $x=0$.

in Fig. 1 that a small addition of Pd to Au causes no substantial effects on the quantized conductance peaks in Au. The histogram of $x=0.17$ is nearly identical to that of pure Au. This observation is consistent with previous experiments by Hansen *et al.*⁴ who also found that the conductance histogram of Au-5-wt. %Co is almost the same as that of pure Au. These results indicate that dilute alloying of Au does not destroy the quantized conductance of Au. Upon increasing the Pd concentration, the $2G_0$ and higher peaks first disappear at $x=0.32$. However, the $1G_0$ peak survives, and remains at the quantized position. At $x=0.55$, the $1G_0$ peak is further reduced, but still visible above the background. It appears as a tiny maximum at $x=0.65$, and becomes hardly identified at $x=0.88$. At the same time, a broad feature starts to grow at $x=0.88$, and dominates the histogram at $x=0.97$. This structure resembles broad peaks observed in Pt, Ru, and Rh,¹⁶ and perhaps has the same origin, which is not well understood at this time. In pure Pd, however, the histogram shows no structures, in agreement with our previous experiment.¹⁶ Similar changes were also observed in conductance histograms at 400 mV, though the broad structure at $x=0.97$ is severely smeared out.

We focus our attention on the behavior of the $1G_0$ peak, and in Fig. 2 plot its position and height as functions of the Pd concentration. These peak parameters were obtained by

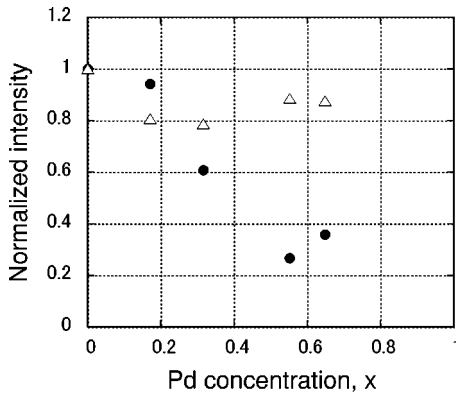


FIG. 3. Concentration dependence of the average $1G_0$ plateau length (open triangles) and the $1G_0$ plateau appearance probability (closed circles). Both data are normalized by their values at $x=0$.

subtracting a background and making a Gaussian fit to the $1G_0$ peak. We could not make a good peak fitting for $x=0.88$ and 0.97 , and in Fig. 2 only show fitting results for $x \leq 0.65$. Note that each peak height in Fig. 2(b) is normalized by its value in pure Au ($x=0$). An interesting observation in Fig. 2(b) is that the $1G_0$ peak position shows no shift upon alloying, and remains within $0.95G_0-1G_0$. Peak positions slightly lower than $1G_0$ are observed even in pure Au, and are usually attributed to the residual resistance.¹⁸ If we treat Pd solute atoms simply as random scattering centers (or disorders), we would expect an appreciable shift of the $1G_0$ peak, as predicted by theoretical calculations.^{18,19} However, no such peak shift with alloying was actually observed. This result suggests that Pd atoms in Au-Pd nanocontacts do not behave as weak scatterers. We will discuss this point in Sec. IV.

In contrast to the peak position, the $1G_0$ peak height shows an appreciable concentration dependence and decreases with increasing Pd concentration. If the $1G_0$ peak height of $Au_{1-x}Pd_x$ is simply a compositional average of those of Au and Pd, then the normalized peak height should decrease as $1-x$ because the $1G_0$ peak height of Pd is effectively zero. Data points in Fig. 2(b), however, fall below $1-x$, and do not fit a linear interpolation. In our previous paper,²⁵ we pointed out that the $1G_0$ peak height is proportional to two factors: the average length Λ and the formation probability p of $1G_0$ plateaus. To investigate which of these factors dominates the concentration dependence of the $1G_0$ peak height, or if they both do, we calculated $\Lambda(x)$ and $p(x)$ from our experimental data. In these calculations, we counted the number of well-defined $1G_0$ plateaus which last 400 ns or longer, and took a conductance value agreeing with the $1G_0$ peak position within $\pm 0.05G_0$. The results are summarized in Fig. 3, where relative changes in $\Lambda(x)$ and $p(x)$ with respect to their values at $x=0$ are plotted. The average plateau length first decreases at $x=0.17$, but then shows little variation upon further increasing the Pd concentration. On the other hand, the formation probability decreases with increasing x and exhibits a behavior simulation to that of the $1G_0$ peak height. By comparing Figs. 3(b) and 2(b), it is evident that the formation probability $p(x)$ determines the

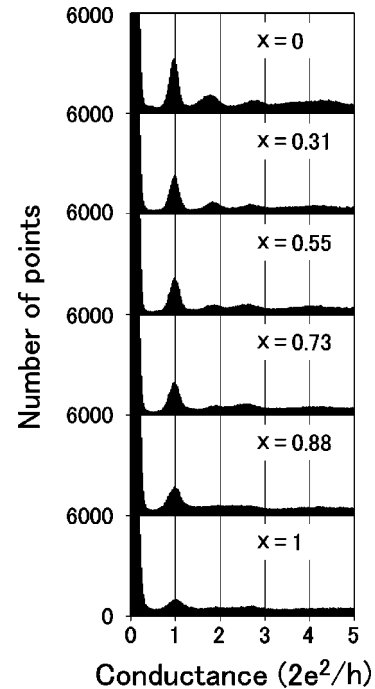


FIG. 4. Conductance histograms of $Au_{1-x}Ag_x$ obtained at 200 mV.

concentration dependence of the $1G_0$ peak height. We note that a close correlation between $p(x)$ and the $1G_0$ peak height is also observed in the bias dependence of the $1G_0$ peak in pure Au.²⁵

B. Au-Ag contacts

Figure 4 shows observed conductance histograms of $Au_{1-x}Ag_x$ nanocontacts at 200 mV. As in the case of Au-Pd, each histogram was constructed from 2000 conductance traces. Different from Pd, pure Ag displays a well-defined $1G_0$ peak. As a result, a clear $1G_0$ peak is observed in all histograms. Conductance peaks at $2G_0$ and $3G_0$ are resolved up to $x=0.55$, but then merge into a broad structure for higher Ag concentrations. This broad structure exists in the histogram of pure Ag in Fig. 4, but becomes hardly visible in the vertical scale of the histogram. Our conductance histogram of pure Ag is in good agreement with those in previous experiments,^{3,4} but shows the $1G_0$ peak having a considerably smaller height than that of Au. The smaller $1G_0$ peak in Ag may be due to the relatively higher mechanical hardness of Ag than Au, since harder metals tend to exhibit the $1G_0$ conductance less clearly.¹⁶

We calculated the position and height of the $1G_0$ peak, and plot them in Fig. 5. As in the case of Au-Pd, the peak position shows a weak concentration dependence, and all data points lie between $0.95G_0$ and $1G_0$. The $1G_0$ peak height decreases with increasing Ag concentration. However, it does not vanish, and takes a nonzero value at $x=1$. The dashed line in Fig. 5(b) represents a linear interpolation between the values of pure Au and Ag. As seen in the figure, the dashed line fits the data points well. This result indicates that the $1G_0$ conductance in Au-Ag is simply a linear compositional average of those of Au and Ag.

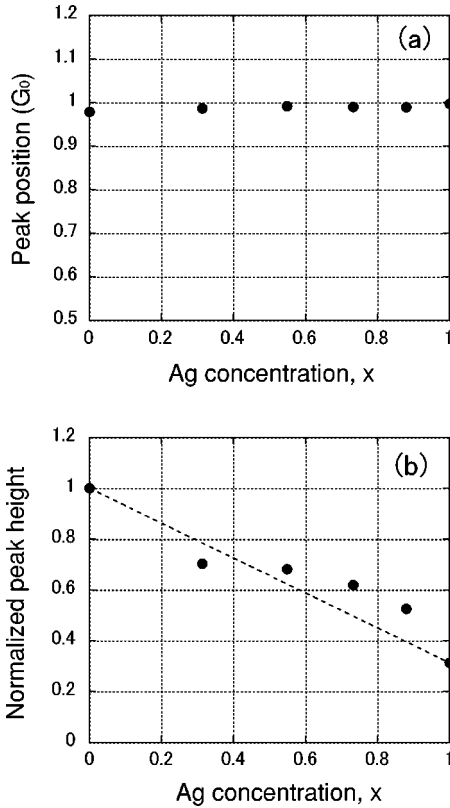


FIG. 5. Peak position (a) and peak height (b) of the $1G_0$ conductance peak of $\text{Au}_{1-x}\text{Ag}_x$ plotted against the Ag concentration. The peak height is normalized by its value at $x=0$. The dashed line in (b) represents a linear interpolation between the peak heights of pure Au and Ag.

IV. DISCUSSION

Our experimental results on Au-Pd and Au-Ag alloy nanocontacts revealed two alloying effects on the $1G_0$ conductance. One is the absence of a peak shift upon alloying, as clearly demonstrated in Figs. 2(a) and 5(a). Another effect is the observed concentration dependence of the peak height shown in Figs. 2(b) and 5(b). In particular, in Au-Pd alloys, the $1G_0$ peak disappears for $x \geq 0.88$. Before discussing these alloying effects, we first consider an atomic geometry of the $1G_0$ contact of Au. In breaking contacts, the $1G_0$ state may not be unique, and will take different geometries each time it appears. It is, however, probable that some contact geometries have higher stabilities than others, and appear more frequently. Since we are dealing with the $1G_0$ peak formed by accumulating many $1G_0$ conductance data, these “statistically preferred” geometries are the relevant contact geometry to our analysis. According to previous experiments such as force measurements,^{26,27} direct transmission electron-microscopy (TEM) observations,^{28–32} and computer simulations,^{27,33,34} a single-atom contact can be the likeliest candidate for the stable $1G_0$ contact of Au. There is a variety of atomic geometries among the single-atom contact of Au, ranging from a one-atom contact to a nine-atom chain bridging between electrodes.³¹ Also, the contact geometry depends on crystallographic orientations.^{33,34} In our experiment, we have no control on the orientation of our contacts.

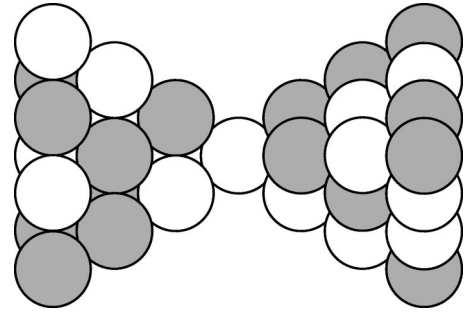


FIG. 6. A model for the $1G_0$ contact of $\text{Au}_{1-x}\text{Pd}_x$.

However, Rodrigues *et al.*³² showed that, in breaking Au contacts, $\langle 111 \rangle$ - and $\langle 100 \rangle$ -oriented structures are statistically favored for the $1G_0$ contact. These structures are likely one- or two-atom chains, as suggested by TEM observations²⁹ and computer simulations.^{33,34} Based on these results, we model the $1G_0$ contact as a one-atom contact attached to $\langle 111 \rangle$ electrodes, as shown in Fig. 6. This does not mean that we exclude all other contact geometries. Rather, we employ the structure of Fig. 6 as a working model for the majority of contacts contributing to the $1G_0$ peak.

Now we consider alloying effects. In Au-Pd contacts, a contact site is not always occupied by Au atoms but sometimes by Pd atoms, the probability of which depends on the Pd concentration. When a Pd atom replaces a Au atom in a $1G_0$ single-atom chain, the Pd atom should reflect electrons and decrease the $1G_0$ conductance to $(1-R)G_0$, where R represents an electron reflection probability. If R is small and constant, this reduced conductance would shift the $1G_0$ peak or form a subpeak at $(1-R)G_0$ in a conductance histogram. However, neither peak shift nor subpeaks were observed in our histograms in Fig. 1. This means that R is either ~ 1 or is too varied to form a subpeak. The latter is unlikely, since $1G_0$ plateau positions in conductance traces do not vary so much. This leads to $R \sim 1$ for Pd. As we mentioned in Sec. I, valence electrons of Pd have a strong d character, and should have a poor matching with the sp conductance channels of neighboring Au atoms. It is thus likely that a Pd atom in a Au single-atom chain cuts off the conductance channel, similar to an S atom in an Al chain studied by Lang.²¹ All $1G_0$ peaks in Au-Pd histograms in Fig. 1 can then be due to pure Au contacts containing no Pd atoms. We note that a formation of pure Au contacts was already considered by Hansen *et al.*⁴ for explaining observed nG_0 peaks in Au-5-wt.%Co contacts.

As we discussed in Sec. III A, the concentration dependence of the $1G_0$ peak height in Au-Pd is determined by that of the formation probability $p(x)$ of $1G_0$ contacts. According to the above argument, this p should be a probability of finding pure-Au $1G_0$ contacts. Since our experimental data in Figs. 2(b) and 3(b) are normalized by the values of pure Au, we also consider $p(x)$ as normalized by its value at $x=0$. Therefore, $p(0)=1$ in pure Au. As the Pd concentration increases, the formation of pure Au contacts becomes less probable, and $p(x)$ decreases with increasing x . The observed reduction of the peak height in Fig. 2(b) directly reflects this decrease in $p(x)$. Unfortunately, it is not easy to

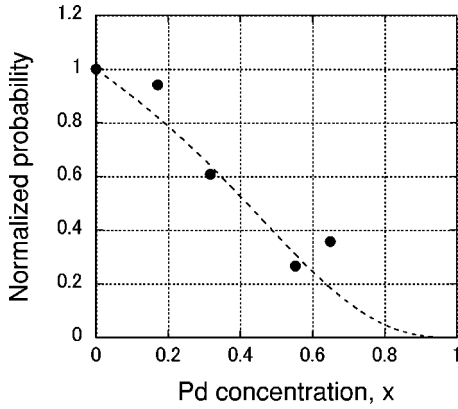


FIG. 7. Comparison of the $1G_0$ plateau appearance probability (closed circles) of $Au_{1-x}Pd_x$ to the formation probability (dashed curve) of pure Au links in the model contact of Fig. 6.

estimate $p(x)$, since it critically depends on details of deformation processes of Au-Pd nanocontacts, which are not clarified at all. Computer simulations of favored contact geometries³⁴ and detailed calculations on the deformation processes of nanocontacts^{27,33} would be necessary to accurately determine $p(x)$. Here we assume a simple atomic geometry for the $1G_0$ contact shown in Fig. 6, and calculate $p(x)$ as a configurational probability of forming an all-Au atomic link between electrodes. In this model, the contact atom has three neighbors in the top atomic layer of each electrode. For obtaining a pure Au contact, the contact atom must be Au. This occurs with a probability $1-x$. However, this condition is not sufficient since, when the Au contact atom has only Pd neighbors in either electrode, then the conductance channel of Au would be disrupted in the top layer of the electrode. Therefore, we have to assume that, in both electrodes, at least one of three neighbor atoms touching the contact atom should be Au (the second and deeper layers of the electrodes are treated as bulk). This second condition gives a nonlinear factor $(1-x^3)^2$. The total probability of forming a Au atomic link between electrodes can then be written as $p(x) = (1-x)(1-x^3)^2$. In Fig. 7, we compare this $p(x)$ with our experimental data shown in Fig. 3. As seen in the figure, $p(x)$ decreases linearly as $1-x$ for small x , but gradually falls below it. This behavior of $p(x)$ well reproduces the concentration dependence of the experimental probability of $1G_0$ plateau formation. This agreement supports our assumption that the $1G_0$ conductance in Au-Pd nanocontacts is due to the formation of all-Au atomic links.

A couple of comments should be addressed to our calculation of $p(x)$. First, the probability $p(x)$ is model dependent. If we have two or three contact atoms in a parallel configuration, for example, a resulting $p(x)$ vanishes at $x=0,1$ and exhibits a maximum at around $x \sim 0.5$. Also, if we arrange contact atoms in the form of a single alloy chain, $p(x)$ decreases more rapidly, and shows worse agreement with the experiment. Therefore, our explanation of experimental results in terms of $p(x)$ would not be justified if these geometries are the most typical $1G_0$ contact geometries. There is, however, no evidence to verify their strong statistical preference in Au and Au-Pd nanocontacts. Their contri-

butions to $p(x)$ thus seems not to be very important. We note, however, that a probability quite similar to our $p(x)$ can be obtained on a one-atom contact with the $\langle 100 \rangle$ orientation. Also, a single-chain contact yields exactly the same probability as our $p(x)$, if its chain atoms are all Au. We cannot discriminate contributions to $p(x)$ from these contact geometries.

A second comment can be made about the alloy composition in nanocontacts. It is quite likely that the composition of each alloy nanocontact differs from a bulk value, and shows a large fluctuation. However, we expect that an average composition over many nanocontacts should be close to the bulk value. Since we are dealing with behaviors of conductance peaks constructed from a large number of data, the use of the bulk value as the alloy composition of nanocontacts may be a reasonable first approximation.

In bulk Au-Pd alloys, the Pd d band starts to cross the Fermi level at $x \sim 0.45$, and makes a significant contribution to the Fermi-level density of states (DOS) for higher Pd concentrations.^{22,23} In Fig. 1, a broad structure appears at $x = 0.65$, and grows with the Pd concentration. The emergence of this broad structure is probably related to the gradual dominance of the Pd- d states in the Fermi level DOS in Au-Pd. We note that similar broad peaks are also observed in some transition-metal nanocontacts.^{15,16} The Pd d -band contribution to the Fermi level DOS is negligible for low Pd concentrations, but increases with a sharp threshold around $x \sim 0.45$. Therefore, this concentration dependence of the Pd- d states cannot be the source of the observed reduction of the $1G_0$ peak height.

In Au-Ag alloy nanocontacts, the appearance of the $1G_0$ conductance is more favored than in Au-Pd. Different from Pd, Ag has a transmitting sp channel and shows a clear $1G_0$ peak in its histogram. Also, Au-Ag alloys have sp electrons at the Fermi level over the entire range of Ag concentration. Therefore, in a one-atom contact of Au-Ag, an open sp conductance channel should always exist, regardless of whether the contact atom is Au or Ag. In this case, the (normalized) formation probability of the $1G_0$ contact simply becomes a concentration-weighted average $p(x) = \alpha x + (1-x)$, where x now stands for the Ag concentration, and α is the ratio of the $1G_0$ peak height of Ag to that of Au. As we can see in Fig. 5(b), this linear interpolation is in good agreement with the experiment.

The above discussion is based on a rather naïve interpretation of conductance channels in terms of valency, or orbital characters of electrons, the validity of which appears to be well established for pure metal nanocontacts.^{6-8,17} We simply applied the valency model to alloy conductance channels, and considered that the $1G_0$ conductance channel of Au should be disrupted by Pd atoms because of their small sp -like DOS, but not by Ag atoms which have sp -like states at the Fermi level. Although this simple interpretation is consistent with our experimental results on Au-Pd and Au-Ag, a real understanding of alloy conductance channels is impossible in the absence of elaborate electronic structure calculations of alloy nanocontacts. We hope that our experimental results will provide motivation for such calculations.

Note added in proof. Recent experiments³⁵ carried out at 4.2 K showed that Pd nanocontacts exhibit very short conductance plateaus. We could not observe these plateaus, perhaps because our experiments were conducted at room temperature.

V. CONCLUSION

To study the effect of alloying on the quantized conductance in Au nanocontacts, we added Pd and Ag into Au, and investigated how the $1G_0$ quantized conductance changes upon alloying. It is found that the $1G_0$ peak in conductance histogram is well observed in both alloys. In Au-Ag, the $1G_0$ peak appears for all Ag concentrations, and, in Au-Pd, it

survives at least in Au-rich nanocontacts. Neither peak shift nor subpeaks are observed. In the case of Au-Pd, Pd atoms are likely to act as a blocking element of the sp conductance channel of Au because of their small sp valency. Then, a formation of an all-Au atomic link is necessary for obtaining the $1G_0$ conductance. Assuming a simple one-atom contact geometry, we calculated a chance of finding an all-Au link, and showed that its concentration dependence consistently explains the observed behavior of the $1G_0$ peak height. On the other hand, in Au-Ag, Ag atoms do not form a bottleneck of the $1G_0$ conductance channel, and the $1G_0$ peak height can be well described as a linear average of those of pure Au and Ag.

*Present address: Toyota Motors Co.

†Corresponding author. Email address: sakai@mesostm.mtl.kyoto-u.ac.jp

¹*Nanowires*, Vol. 340 of *NATO Advanced Study Institute, Series E: Applied Physics*, edited by P. A. Serena and N. García (Kluwer, Dordrecht, 1997).

²M. Brandbyge, J. Shiótz, M. R. Sørensen, P. Stolze, K. W. Jacobsen, J. K. Nørskov, L. Olesen, E. Lægsgarrd, I. Stensgaard, and F. Besenbacher, *Phys. Rev. B* **52**, 8499 (1995).

³J. L. Costa-Krämer, N. García, P. García-Mochales, P. A. Serena, M. I. Marqués, and A. Correia, *Phys. Rev. B* **55**, 5416 (1997).

⁴K. Hansen, E. Lægsgarrd, I. Stensgaard, and F. Besenbacher, *Phys. Rev. B* **56**, 2208 (1997).

⁵J. L. Costa-Krämer, N. García, P. García-Mochales, M. I. Marqués, and P. A. Serena, in *Nanowires* (Ref. 1), p. 171.

⁶J. C. Cuevas, A. Levy Yeyati, A. Martín-Rodero, G. Rubio Bollinger, C. Untiedt, and N. Agraït, *Phys. Rev. Lett.* **81**, 2990 (1998).

⁷M. Brandbyge, N. Kobayashi, and M. Tsukada, *Phys. Rev. B* **60**, 17064 (1999).

⁸K. Hansen, S. K. Nielsen, M. Brandbyge, E. Lægsgarrd, I. Stensgaard, and F. Besenbacher, *Appl. Phys. Lett.* **77**, 708 (2000).

⁹E. Scheer, N. Agraït, J. C. Cuevas, A. Levy Yeyati, B. Ludoph, A. Martín-Rodero, G. Rubio-Bollinger, J. M. van Ruitenbeek, and C. Urbina, *Nature (London)* **395**, 780 (1998).

¹⁰F. Ott, S. Barberan, J. G. Lunney, J. M. D. Coey, P. Berthet, A. M. de Leon-Guevara, and A. Revcolevschi, *Phys. Rev. B* **58**, 4656 (1998).

¹¹H. Oshima and K. Miyano, *Appl. Phys. Lett.* **73**, 2203 (1998).

¹²T. Ono, Y. Ooka, H. Miyajima, and Y. Otani, *Appl. Phys. Lett.* **75**, 1622 (1999).

¹³F. Komori and K. Nakatsuji, *J. Phys. Soc. Jpn.* **68**, 3786 (1999).

¹⁴J. L. Costa-Krämer, *Phys. Rev. B* **55**, R4875 (1997).

¹⁵B. Ludoph and J. M. van Ruitenbeek, *Phys. Rev. B* **61**, 2273 (2000).

¹⁶K. Yuki, S. Kurokawa, and A. Sakai, *Jpn. J. Appl. Phys.* **40**, 803 (2001).

¹⁷J. C. Cuevas, A. Levy Yeyati, and A. Martín-Rodero, *Phys. Rev. Lett.* **80**, 1066 (1998).

¹⁸P. García-Mochales and P. A. Serena, *Phys. Rev. Lett.* **79**, 2316 (1997).

¹⁹J. Bürki, C. A. Stafford, X. Zotos, and, D. Baeriswyl, *Phys. Rev. B* **60**, 5000 (1999).

²⁰M. Brandbyge, K. W. Jacobsen, and J. K. Nørskov, *Phys. Rev. B* **55**, 2637 (1997).

²¹N. D. Lang, *Phys. Rev. B* **52**, 5335 (1995).

²²P. M. Laufer and D. A. Papaconstantopoulos, *Phys. Rev. B* **35**, 9019 (1987).

²³P. Weinberger, L. Szunyogh, and B. I. Bennett, *Phys. Rev. B* **47**, 10154 (1993).

²⁴H. Yasuda and A. Sakai, *Phys. Rev. B* **56**, 1069 (1997).

²⁵K. Itakura, K. Yuki, S. Kurokawa, H. Yasuda, and A. Sakai, *Phys. Rev. B* **60**, 11163 (1999).

²⁶G. Rubio, N. Agraït, and S. Vieira, *Phys. Rev. Lett.* **76**, 2302 (1996).

²⁷G. Rubio-Bollinger, S. R. Bahn, N. Agraït, K. W. Jacobsen, and S. Vieira, *Phys. Rev. Lett.* **87**, 026101 (2001).

²⁸H. Ohnishi, Y. Kondo, and K. Takayanagi, *Nature (London)* **395**, 780 (1998).

²⁹H. Ohnishi, Y. Kondo, and K. Takayanagi (unpublished).

³⁰T. Kizuka *Phys. Rev. Lett.* **81**, 4448 (1998).

³¹T. Kizuka, S. Umehara, and S. Fujisawa, *Jpn. J. Appl. Phys.* **40**, L71 (2001).

³²V. Rodrigues, T. Fuhrer, and D. Ugarte, *Phys. Rev. Lett.* **85**, 4124 (2000).

³³M. R. Sørensen, M. Brandbyge, and K. Jacobsen, *Phys. Rev. B* **57**, 3283 (1998).

³⁴A. Hasmy, E. Medina, and P. A. Serena, *Phys. Rev. Lett.* **86**, 5574 (2001).

³⁵R. H. M. Smit, C. Untiedt, A. I. Yanson, and J. N. van Ruitenbeek, *Phys. Rev. Lett.* **87**, 266102 (2001).